PERGAMON

International Journal of Solids and Structures 40 (2003) 5407–5422

INTERNATIONAL JOURNAL OF SOLIDS and STRUCTURES

www.elsevier.com/locate/ijsolstr

Analysis for polycrystal nonproportional cyclic plasticity with a dissipated energy based rule for cross-hardening

X. Peng *, J. Fan

Department of Engineering Mechanics, Chongqing University, Chongqing, 400044, People's Republic of China

Received 5 August 2002; received in revised form 20 April 2003

Abstract

Based on a nonclassical hardening law and the Hill's self-consistent scheme, a new approach is proposed for the analysis of polycrystal nonproportional cyclic plasticity. A novel parameter related to the plastic dissipation on each slip system is proposed and embedded in the Bassani's definition of cross-hardening. The tangential elastoplastic tensor relating the increments of stress and strain in a single crystal is derived and the corresponding numerical algorithm for polycrystal plasticity is developed. The elastoplastic response of 316 stainless steel subjected to typical biaxial nonproportional strain cycling is analyzed, and the main features are well replicated. The validity of the proposed approach is demonstrated by the satisfactory agreement between the computed results and experimental observation.

Keywords: Crystal plasticity; Hardening law; Hill's self-consistent scheme; Polycrystal; Nonproportional cyclic plasticity

1. Introduction

The research on constitutive models for nonproportional cyclic plasticity is of great importance in the stress analysis and life prediction for structures and machine components subjected to severe loading conditions. This is mainly due to the fact that stress and strain generally distribute nonuniformly and vary nonproportionally, and the low-cycle fatigue life under nonproportional cyclic loading is much less than in the proportional cases (Krempl and Lu, 1987; Brown and Miller, 1982).

In the past two decades, various constitutive descriptions have been proposed for the cyclic plasticity of polycrystalline materials, such as those by Ohno (1982), Chaboche and Rousselier (1983), McDowell (1985), Sotolongo and McDowell (1986), Krempl and Lu (1987), Benallel and Marquis (1987), Murakami et al. (1989), McDowell (1987), Moosbrugger and McDowell (1989), Bassani (1990), Fan and Peng (1991), Tanaka (1994), Peng and Ponter (1994), Hwang and Sun (1994), Peng et al. (1997), and Peng and Fan (2000). Among these descriptions, those based on the slip mechanism of single crystals and self-consistent schemes (Bassani, 1990; Hwang and Sun, 1994; Peng et al., 1997; Peng and Fan, 2000) are of special interest

* Corresponding author. Tel.: +86-23-6510-3755; fax: +86-23-6511-1468/6410-6656.
E-mail address: xhpeng@cqu.edu.cn (X. Peng).

0020-7683/$ - see front matter
doi:10.1016/S0020-7683(03)00284-1

due to the attempt to gain insight into the hardening behavior of polycrystalline materials under non-proportional cyclic loading.

Great progress has been achieved in crystal plasticity since it was firstly proposed by Taylor (1938) and extended by Bishop and Hill (1951). Lin (1957) extended Taylor's model to include elastic strain. Kroner (1961), and Budiansky and Wu (1962) proposed a model that specified a self-consistent scheme for calculating the overall stress-strain behavior of a polycrystal by taking into account the interaction between crystals in a particular way. With the development of the Hill's self-consistent scheme, a more general system related to the geometry and kinetics of crystal plasticity was completed (Hill, 1966; Hill and Rice, 1972). In the past decades, the Hill's self-consistent scheme received increasing attention and be applied to various problems (Hutchinson, 1970; Berveiller and Zaoui, 1979; Fan, 1999).

Meanwhile, progress was also made in the description of the constitutive behavior of slip systems and crystals. The conventional constitutive relationship of a slip system was derived within the framework of the conventional theory of plasticity, i.e., taking the existence of a critical shear stress as its premise. The activation of a slip system depends on this critical shear stress and the corresponding slip criterion. A new slip model and the corresponding hardening law were recently proposed by Peng et al. (1997), and Peng and Fan (2000), alternatively, which takes into account the contribution of the energy stored in the microstructure of a plastically deformed material to the subsequent plastic deformation. It does not use the concept of a critical shear stress and the corresponding slip criterion. The corresponding analysis, therefore, is greatly simplified because it involves no additional process for the determination of the activation of slip systems and the direction of slip. The corresponding approach based on the KBWs self-consistent scheme was developed and applied to the nonproportional cyclic plasticity of polycrystalline materials (Peng et al., 1997; Peng and Fan, 2000).

In this paper, a new approach for polycrystal plasticity is developed based on the nonclassical hardening law (Peng et al., 1997; Peng and Fan, 2000) and the Hill's self-consistent scheme. A new parameter related to the plastic dissipation on each slip system is introduced and embedded in the Bassani's definition for cross-hardening, which greatly improves the description for nonproportional cyclic plasticity. The tangential elastoplastic tensor relating the increments of stress and strain in a single crystal is proposed and the corresponding numerical algorithm for polycrystal plasticity is developed. The elastoplastic responses of 316 stainless steel subjected to cycling along typical proportional and biaxial nonproportional paths are analyzed, and the main characteristics of polycrystal nonproportional cyclic plasticity are well described compared with experimental results (Murakami et al., 1989; Ohashi et al., 1985).

2. A brief introduction to the nonclassical hardening law

In polycrystalline materials, the deformation of any single crystal is inevitably constrained by the neighboring crystals due to the nonhomogeneous morphology of the materials, which may result in residual microstress fields. On the other hand, in a plastically deformed single crystal, there also exist residual microstress fields in the stochastic microstructures due to the nonhomogeneous nature and the respective pattern of lattice defects, for instance, dislocations (Song, 1992). The energy stored in the residual microstress fields may contribute to the subsequent plastic deformation. With this concept, a hardening law was proposed for single crystals (Peng et al., 1997; Peng and Fan, 2000) as follows:

$$\dot{\tau}^{(m)} = \sum_{n=1}^{N} h_{mn}\dot{\gamma}^{(n)} \quad (m = 1, 2, \ldots, N), \tag{1}$$

where $\gamma^{(m)}$ and $\tau^{(m)}$ denote the slip amount and the shear stress on the mth slip system; N, the number of the independent slip systems; δ_{mn}, the Kronecker symbol and h_{mn}, the hardening coefficient expressed as

$$h_{mn} = T_m \delta_{mn} \quad (m \text{ not summed}), \tag{2}$$

with

$$T_m = C - \frac{\alpha \Gamma_m}{f_m H_m} \tau^{(m)}, \quad \Gamma_m = \frac{\mathrm{d}\gamma^{(m)}}{\mathrm{d}\zeta^{(m)}} \quad (m \text{ not summed}), \tag{3}$$

C and α are material dependent parameters. f_m and H_m are hardening functions describing respectively instantaneous hardening related to the slip on the mth slip system, and cross-hardening related to the interaction between the slips on different slip systems (Bassani, 1990). It can be proved that h_{mn} is positively definite if $f_m H_m$ is positive and nondecreasing, which guarantees the existence and uniqueness of the solution. $\zeta^{(m)}$ is the accumulated slip on the mth slip system defined by

$$\mathrm{d}\zeta^{(m)} = |\mathrm{d}\gamma^{(m)}|, \tag{4}$$

which is nondecreasing and can be used as generalized time to measure the slip history of the mth slip system. In order to simplify the nonlinear analysis, an intrinsic time, originally proposed by Valanis (1980), was introduced to describe the plastic deformation history on the mth slip system as follows:

$$\mathrm{d}z^{(m)} = \frac{\mathrm{d}\zeta^{(m)}}{f_m H_m} \quad (m \text{ not summed}). \tag{5}$$

With this definition and making use of Eqs. (1)–(3), the evolution of the shear stress on the mth slip system can be expressed as

$$\mathrm{d}\tau^{(m)} = C\,\mathrm{d}\gamma^{(m)} - \alpha \tau^{(m)}\,\mathrm{d}z^{(m)} \quad (m \text{ not summed}, \ m = 1, \ldots, N). \tag{6}$$

It is worthwhile to emphasize that this slip model does not use the concept of a critical shear stress, due to the consideration of the contribution of the energy stored in the residual microstress fields to the subsequent plastic deformation. However, the critical shear stress, as used in the conventional slip model, can be obtained as a special case from the above slip model by assuming α tends to infinite while C/α remains limited (Peng and Fan, 2000)

$$\tau_m = \pm a_0 f_m H_m \quad (m \text{ not summed}), \tag{7}$$

where $a_0 = C/\alpha$ represents the initial critical shear stress. Eq. (7) can be also equivalently derived from the model without taking into account the energy stored in the residual microstress fields and its contribution to subsequent plastic deformation (Peng and Fan, 2000).

3. Physically based hardening functions

In Eq. (3), hardening functions f_m and H_m are introduced to describe respectively the instantaneous hardening related to dislocation pile-ups, and the cross-hardening related to dislocation tangles. During plastic deformation, obstacles formed by the pile-ups and tangles of dislocations increase the resistance to active dislocations and result in macroscopic hardening.

Dislocation pile-ups induce long-range residual microstress fields, which are directional and thus kinematic, accounting for the Bauschinger effect to some extent. The hardening of a slip system induced by dislocation pile-ups should be, therefore, determined by the superposition of the effects of the corresponding residual microstress fields caused by dislocation pile-ups in all slip systems.

The hardening related to dislocation tangles can be attributed to the interaction between the active dislocations and dislocation forests. The associated residual microstress fields are of short-range and less directional. This type of hardening depends strongly on slip histories and the states of dislocation on all slip systems. On the other hand, the interaction between dislocations from different slip systems may make different contribution to hardening.

Suppose f_m possesses a saturated value corresponding to the saturated state of dislocation, the evolution of f_m with respect to intrinsic time $z^{(m)}$ should be related to the current f_m and may be given approximately the following simple form,

$$\frac{\mathrm{d}f_m}{\mathrm{d}z^{(m)}} = \beta_1(d_1 - f_m) \quad (m = 1, 2, \ldots, N), \tag{8}$$

where d_1 and β_1 are two material parameters representing the saturated value of f_m and the rate for f_m to approach d_1, respectively.

Based on a detailed analysis of cross-hardening mechanisms, Bassani (1990) proposed a hardening rule to describe cross-hardening, and the form of this rule is directly adopted to be the cross-hardening function H_m, i.e.,

$$H_m = 1 + \sum_{k \neq m} \lambda_{mk} \tanh(2\beta_s \zeta^{(k)}) \quad (m = 1, 2, \ldots, N), \tag{9}$$

where $\zeta^{(k)}$ denotes the accumulated slip on the kth slip system, β_s is a material parameter representing the rate for H_m to approach its saturation value, and λ_{mk} is a coupling parameter related to the orientations of the considered two slip systems m and k, taking into account the contribution of the accumulated slip on the kth slip system to the hardening of the mth slip system.

A direct application of Eq. (9) in the current constitutive framework may overestimate the cross-hardening in the case of proportional cyclic loading if f_{mk} is simply composed of a set of constants (Peng et al., 1997; Peng and Fan, 2000). It is known that the summation of the dissipated energy on all slip systems equals the energy dissipated during the corresponding macroscopic plastic deformation. Compared with a proportional cyclic loading, it can be found that more energy is dissipated during nonproportional cyclic loading since it may involve less unloading and plastic deformation may develop at a higher level of stress. Consequently, it may induce stronger residual microstress fields and more energy stored in the microstructures, which accounts for the cross-hardening in materials. With this concept a dissipated energy ratio for the mth slip system is defined as follows:

$$\xi^{(m)} = \frac{\eta^{(m)}}{A_m \zeta^{(m)}}, \tag{10}$$

in which

$$\eta^{(m)} = \int \tau^{(m)} \, \mathrm{d}\gamma^{(m)} \quad (m \text{ not summed}) \tag{11}$$

denotes the energy dissipated on the mth slip system, A_m is the parameter related to material property and the current state of instantaneous hardening, f_m. If $A_m = f_m C/\alpha$, as used in the analysis, the denominator on the right-hand side of Eq. (10) represents a bound of the dissipated energy on the mth slip system under the condition of $H_m = 1$, i.e., without taking into account the cross-hardening (see Appendix A). It will be seen that the combination of this dissipated energy ratio and Bassani's hardening rule can yield a satisfactory description for additional nonproportional hardening.

With the proposed dissipated energy ratio, the coupling coefficients λ_{mn} (Eq. (9)) can be defined as follows:

$$\lambda_{mn} = g_{mn} \xi^{(m)} \xi^{(n)} \quad (m, n = 1, 2, \ldots, N; \ m, n \text{ not summed}), \tag{12}$$

where g_{mn} can be expressed in the following matrix form (Bassani, 1990), with the sequence identical with that of the 12 independent slip systems (see Table 3):

$$[g_{mn}] = \begin{bmatrix} 0 & c_1 & c_1 & c_3 & c_2 & c_1 & c_1 & c_2 & c_2 & c_1 & c_3 & c_2 \\ & 0 & c_1 & c_2 & c_1 & c_2 & c_1 & c_3 & c_1 & c_3 & c_1 & c_2 \\ & & 0 & c_1 & c_2 & c_3 & c_2 & c_1 & c_3 & c_2 & c_2 & c_1 \\ & & & 0 & c_1 & c_1 & c_2 & c_1 & c_2 & c_2 & c_3 & c_1 \\ & & & & 0 & c_1 & c_3 & c_2 & c_1 & c_2 & c_1 & c_3 \\ & & & & & 0 & c_1 & c_2 & c_3 & c_1 & c_2 & c_2 \\ & & & & & & 0 & c_1 & c_1 & c_1 & c_2 & c_3 \\ & & & & & & & 0 & c_1 & c_3 & c_2 & c_2 \\ & & \text{sym.} & & & & & & 0 & c_2 & c_1 & c_1 \\ & & & & & & & & & 0 & c_1 & c_1 \\ & & & & & & & & & & 0 & c_1 \\ & & & & & & & & & & & 0 \end{bmatrix}, \tag{13}$$

where c_1, c_2 and c_3 are material constants. It can be seen that the coupling between the dislocation states on two slip systems is introduced into the cross-hardening via λ_{mn} by taking into account the dissipated energy ratios on these two slip systems. In general, the dissipated energy ratio is smaller and the corresponding cross-hardening is insignificant under proportional loading. The dissipated energy ratio may increase remarkably in the case of nonproportional loading, which may result in strong cross-hardening. It will be seen that the proposed hardening parameter λ_{mn} can effectively distinguish the nonproportional hardening corresponding to different types of strain paths.

It can be seen that there exist saturated values d_1 and $1 + \sum_{k\neq m} \lambda_{mk}$ for f_m and H_m respectively. It can be shown that the shear stress on a slip system has a saturated value when plastic deformation fully develops, and the hardening modulus T_m tends to vanish as the shear stress approaches its saturated value.

It is known that besides the cross-hardening corresponding to nonproportional loading, the additional hardening corresponding to cyclic plastic strain range also plays an important role in the cyclic plasticity of metallic materials (Tanaka et al., 1985a; Ohno, 1990; Fan and Peng, 1991). Fan and Peng (1991) introduced a hardening factor, related to the cyclic nonhardening region proposed by Ohno (1982) and Ohno and Kachi (1986), into a multiplicatively separated form of hardening function to describe the effect of plastic strain amplitude. Although in this paper attention is mainly paid to the effect of nonproportionality, we like to mention that the additional hardening related to plastic strain amplitude can also be taken into account by f_m (Eq. (8)), provided the parameter d_1 is related to the amplitude of the slip on each slip system. It will be studied in the further improvement of the proposed model.

4. Hill's self-consistent scheme

In the KBW self-consistent scheme, a crystal is assumed to be embedded in a homogeneous matrix. Hill (1965) and Hutchinson (1970) criticized the KBW model for its elastic matrix and proposed a new self-consistent scheme where the embedded inclusion is subjected to the homogeneous constraint of the matrix associated with overall elastoplastic tangent moduli. The misfit strain between the inclusion and the matrix tends to be absorbed locally in the surrounding matrix. Therefore, the constraint tensor for the outer phase may not be homogeneous and the self-consistent scheme is based on the assumption of uniform overall constraint tensor (Takahashi et al., 1994). Takahashi (1988) thought that the KBW scheme gives the upper limit of the flow stress, whereas the Hill's scheme gives the lower limit. Takahashi et al. (1994) performed a finite element analysis of elastoplastic behavior of FCC polycrystalline metals with the initial strain method and the successive integration method, and found that the computed results fit the results with the KBW model better compared with the results using the Hill's self-consistent scheme. Peng et al. (1997), Peng and Fan (2000) also analyzed the cyclic plasticity of FCC polycrystalline materials with a new slip model and the KBW scheme, and results obtained are reasonable compared with the experimental results. However, the Hill's self-consistent scheme is to be used in the following analysis, because it is thought that, in general, the Hill's self-consistent scheme may provide more actual result because it employs less assumptions, although it may involve some numerical difficulties due to complicated implicit iteration.

Suppose the considered crystals and polycrystal are plastically incompressible, under the condition of isothermal and small deformation, the Hill's self-consistent scheme (Hill, 1965) gives

$$\mathrm{d}\boldsymbol{\sigma}_{\mathrm{c}} - \mathrm{d}\bar{\boldsymbol{\sigma}} = -\mathbf{L}^{*} : (\mathrm{d}\boldsymbol{\varepsilon}_{\mathrm{c}} - \mathrm{d}\bar{\boldsymbol{\varepsilon}}), \tag{14}$$

where $\mathrm{d}\boldsymbol{\sigma}_{\mathrm{c}}$ and $\mathrm{d}\boldsymbol{\varepsilon}_{\mathrm{c}}$ denote respectively the increments of the stress and strain tensors of a single crystal, $\mathrm{d}\bar{\boldsymbol{\sigma}}$ and $\mathrm{d}\bar{\boldsymbol{\varepsilon}}$ are the increments of the averaging stress and plastic strain of the polycrystal, and $\mathbf{L}^{*}$ is a tangential "constraint" tensor. $\mathbf{L}^{*}$ is determined by

$$\mathbf{L}^{*} = \mathbf{L} : (\mathbf{S}^{-1} - \mathbf{I}_4), \tag{15}$$

where $\mathbf{I}_4$ is the identity tenser of rank 4, $\mathbf{L}$ is the tangential elastoplastic tensor relating $\mathrm{d}\bar{\boldsymbol{\sigma}}$ and $\mathrm{d}\bar{\boldsymbol{\varepsilon}}$ by

$$\mathrm{d}\bar{\boldsymbol{\sigma}} = \mathbf{L} : \mathrm{d}\bar{\boldsymbol{\varepsilon}}, \tag{16}$$

and $\mathbf{S}$ is the Eshelby's tensor. Assuming spherical inclusion, the Eshelby's tensor can be expressed as

$$\mathbf{S} = a\mathbf{I}_2 \otimes \mathbf{I}_2 + b[\mathbf{I}_4 - \mathbf{I}_2 \otimes \mathbf{I}_2] \tag{17}$$

with

$$b = \frac{2(4-5v)}{15(1-v)}, \quad a = 1 - b, \tag{18}$$

and $\mathbf{I}_2$, the identity tenser of rank 2. $\mathrm{d}\bar{\boldsymbol{\varepsilon}}$ is related to $\mathrm{d}\boldsymbol{\varepsilon}_{\mathrm{c}}$ by the following relationship

$$\mathrm{d}\boldsymbol{\varepsilon}_{\mathrm{c}} = \mathbf{A}_{\mathrm{c}} : \mathrm{d}\bar{\boldsymbol{\varepsilon}} \tag{19}$$

with

$$\mathbf{A}_{\mathrm{c}} = [\mathbf{L}^{*} + \mathbf{L}_{\mathrm{c}}]^{-1} : [\mathbf{L}^{*} + \mathbf{L}], \tag{20}$$

and $\mathbf{L}_{\mathrm{c}}$ is the tangential elastoplastic tensor relating $\mathrm{d}\boldsymbol{\sigma}_{\mathrm{c}}$ and $\mathrm{d}\boldsymbol{\varepsilon}_{\mathrm{c}}$ of a single crystal by

$$\mathrm{d}\boldsymbol{\sigma}_{\mathrm{c}} = \mathbf{L}_{\mathrm{c}} : \mathrm{d}\boldsymbol{\varepsilon}_{\mathrm{c}}. \tag{21}$$

Eqs. (19) and (20) give the following invariant for each crystal

$$\mathrm{d}\mathbf{q} = [\mathbf{L}^{*} + \mathbf{L}_{\mathrm{c}}] : \mathrm{d}\boldsymbol{\varepsilon}_{\mathrm{c}} = [\mathbf{L}^{*} + \mathbf{L}] : \mathrm{d}\bar{\boldsymbol{\varepsilon}}, \tag{22}$$

which is important in analysis. Assuming the overall increment of stress $\mathrm{d}\bar{\boldsymbol{\sigma}}$ to be determined by $\mathrm{d}\boldsymbol{\sigma}_{\mathrm{c}}$ of all single crystals through a certain averaging procedure, one obtains the relationship between $\mathrm{d}\bar{\boldsymbol{\sigma}}$ and $\mathrm{d}\bar{\boldsymbol{\varepsilon}}$ as follows:

$$\mathrm{d}\bar{\boldsymbol{\sigma}} = \langle \mathrm{d}\boldsymbol{\sigma}_{\mathrm{c}} \rangle = \langle \mathbf{L}_{\mathrm{c}} : \mathbf{A}_{\mathrm{c}} \rangle : \mathrm{d}\bar{\boldsymbol{\varepsilon}}. \tag{23}$$

Comparing Eq. (23) with Eq. (16) immediately gives

$$\mathbf{L} = \langle \mathbf{L}_{\mathrm{c}} : \mathbf{A}_{\mathrm{c}} \rangle. \tag{24}$$

5. Application and verification

5.1. Tangential elastoplastic modulus of a single crystal

It was pointed out that when α is very large, extending Eq. (6) directly to an incremental form would result in a large error in numerical analysis and even affect the convergence of the solution (Peng and Fan, 1993). In order to avoid this situation, the integral of Eq. (6) was introduced and the following incremental constitutive equation was derived (Peng and Fan, 2000):

$$\Delta\tau^{(m)} = A_m\,\Delta\gamma^{(m)} + B_m\,\Delta z^{(m)} \quad (m \text{ not summed}), \tag{25}$$

in which

$$\begin{aligned} &A_m = k_m C, \quad B_m = -k_m\alpha\tau^{(m)}(z_n^{(m)}), \quad z^{(m)} = z_n^{(m)} + \Delta z^{(m)} \\ &k_m = \frac{1 - e^{-\alpha\,\Delta z^{(m)}}}{\alpha\,\Delta z^{(m)}}, \quad \Delta z^{(m)} = \frac{\Delta\zeta^{(m)}}{f_m H_m}, \quad \Delta\zeta^{(m)} = |\Delta\gamma^{(m)}| \end{aligned} \qquad (m \text{ not summed}), \tag{26}$$

$z_n^{(m)}$ and $\tau_m(z_n^{(m)})$ denote respectively the intrinsic time and the corresponding shear stress on the mth slip system after the nth increment of loading, with which Eqs. (1)–(3) can be rewritten as

$$\Delta\tau^{(m)} = T_m\,\Delta\gamma^{(m)}, \quad T_m = A_m + \frac{\Gamma_m B_m}{f_m H_m}, \quad \Gamma_m = \frac{\Delta\gamma^{(m)}}{\Delta\zeta^{(m)}} \quad (m \text{ not summed}). \tag{27}$$

The hardening law for the mth single crystal, therefore, can be rewritten as follows:

$$\Delta\tau^{(m)} = \sum_{n=1}^{N} h_{mn}\,\Delta\gamma^{(m)}. \tag{28}$$

It is known that $\Delta\tau^{(m)}$ and $\Delta\gamma^{(m)}$ relate respectively to $\Delta\boldsymbol{\sigma}_c$ and $\Delta\boldsymbol{\varepsilon}_c^p$ of the corresponding single crystal by

$$\Delta\tau^{(m)} = \mathbf{p}_m : \Delta\boldsymbol{\sigma}_c, \quad \Delta\boldsymbol{\varepsilon}_c^p = \sum_{m=1}^{N} \mathbf{p}_m\,\Delta\gamma^{(m)}, \tag{29}$$

where

$$\mathbf{p}_m = \tfrac{1}{2}(\mathbf{n}_m \otimes \mathbf{s}_m + \mathbf{s}_m \otimes \mathbf{n}_m) \tag{30}$$

denotes the orientation tensor of the mth slip system, $\mathbf{n}_m$ and $\mathbf{s}_m$ are the unit vectors directing along respectively the outer normal of the slip plane and the slip direction.

It has been noted that the hardening tensor h_{mn} is positively definite, Eq. (1), therefore, can be expressed inversely as follows:

$$\Delta\gamma^{(m)} = \sum_{n=1}^{N} b_{mn}\,\Delta\tau^{(n)} \quad (m = 1, 2, \ldots, N). \tag{31}$$

Making use of Eqs. (29) and (31), one obtains

$$\Delta\boldsymbol{\varepsilon}_c^p = \left[\sum_{m=1}^{N}\sum_{n=1}^{N} b_{mn}\mathbf{P}_m \otimes \mathbf{P}_n\right] : \Delta\boldsymbol{\sigma}_c. \tag{32}$$

Substituting

$$\Delta\boldsymbol{\varepsilon}_c = \Delta\boldsymbol{\varepsilon}_c^e + \Delta\boldsymbol{\varepsilon}_c^p \quad \text{and} \quad \Delta\boldsymbol{\varepsilon}_c^e = \mathbf{D}_e^{-1} : \Delta\boldsymbol{\sigma}_c \tag{33}$$

into Eq. (32), where $\Delta\boldsymbol{\varepsilon}_c^e$ and $\mathbf{D}_e$ denote the increment of the elastic strain of a singe crystal and the elastic modulus of the material, one derives the following relationship

$$\Delta\boldsymbol{\sigma}_c = \mathbf{L}_c : \Delta\boldsymbol{\varepsilon}_c \tag{34}$$

with

$$\mathbf{L}_c = \left[\mathbf{D}_e^{-1} + \sum_{m=1}^{N}\sum_{n=1}^{N} b_{mn}\mathbf{P}_m \otimes \mathbf{P}_n\right]^{-1}. \tag{35}$$

The matrix form of this equation is given in Appendix B.

5.2. A mixed averaging procedure

In general, Eq. (24) can be expressed as follows:

$$\mathbf{L} = \frac{1}{V}\sum_{i=1}^{N'}[\mathbf{L}_c : \mathbf{A}_c]_i V_i, \tag{36}$$

where $[\mathbf{L}_c : \mathbf{A}_c]_i$ and V_i represent respectively the $[\mathbf{L}_c : \mathbf{A}_c]$ and the volume of the ith single crystal; V, the volume of the polycrystal and N', the number of the present single crystals. If the volume of each single crystal is assumed identical, i.e., $V = N'V_i$, then Eq. (34) can be rewritten as

$$\mathbf{L} = \frac{1}{N'}\sum_{i=1}^{N'}[\mathbf{L}_c : \mathbf{A}_c]_i. \tag{37}$$

With the assumption that a polycrystal is an aggregate of numerous single crystals with randomly distributed orientations, Eq. (37) can be expressed as an integral and then calculated with the some numerical quadrature approach. This method, in substance, determines approximately the response of a polycrystal using a number of single crystals with specific orientations by weight factors. In order to make the specified orientations distribute as uniformly as possible and make the computation more efficient, a mixed averaging approach was proposed alternatively (Peng et al., 1997; Peng and Fan, 2000) for polycrystal analysis (Peng et al., 1997; Peng and Fan, 2000). It is based on an isosahedron: the outer normal directions of the 20 faces determine 20 spatially uniformly distributed orientations and are represented by 20 sets of θ_i and ϕ_i $(1, 2, \ldots, 20)$, and in each face it is assumed that there are numerous single crystals with randomly distributed orientations, i.e., ω varies continuously (see Fig. 1). If the arithmetic averaging procedure is used for θ_i and ϕ_i $(i = 1, 2, \ldots, 20)$ and the Gaussian averaging for ω, Eq. (37) can be specified as

$$\mathbf{L} = \frac{1}{20}\sum_{i=1}^{20}\frac{1}{2\pi}\int_{-\pi}^{\pi}\mathbf{L}_c(\theta_i, \phi_i, \omega) : \mathbf{A}_c(\theta_i, \phi_i, \omega)\,d\omega. \tag{38}$$

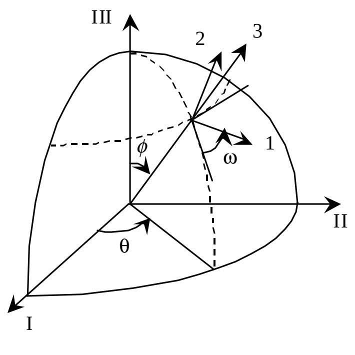

Fig. 1. Global and local coordinate systems.

Table 1
Coordinates of Gaussian points ω_j and the corresponding weight coefficients A_j^{ω}

j	1	2	3	4
ω_j (rad)	0.1090633	0.5183777	1.052419	1.461733
A_j^{ω}	0.3478548	0.6521452	0.6521452	0.3478548

Table 2
Values of the 10 sets of independent θ_j and ϕ_j

j	1	2	3	4	5	6	7	8	9	10
θ_j (°)	0	72	144	216	288	288	216	144	72	0
ϕ_j (°)	37.38	37.38	37.38	37.38	37.38	79.19	79.19	79.19	79.19	79.19

It can be observed that the 20 faces of an isosahedron can be separated into 10 sets, in each of which the two faces are parallel to each other. On the other hand, the integral domain of ω can be reduced to $[0, \pi/2]$ due to symmetry. Applying the Gaussian quadrature to Eq. (36), one obtains

$$\mathbf{L} = \frac{1}{20} \sum_{i=1}^{10} \sum_{j=1}^{4} A_j^{\omega} \mathbf{L}_c(\theta_i, \phi_i, \omega_j) : \mathbf{A}_c(\theta_i, \phi_i, \omega_j), \tag{39}$$

where the coordinates of the Gaussian integration points ω_j and the corresponding weight coefficients A_j^{ω} are given in Table 1, and the values of the 10 sets of independent θ_i and ϕ_i $(i = 1, 2, \ldots, 10)$ are listed in Table 2.

The above averaging procedure involves the responses of 40 single crystals with different orientations, with improvement by the Gaussian weight coefficients. Analysis shows that this mixed procedure can be of satisfactory numerical stability and convergence in the analysis for the elastoplastic responses of polycrystalline materials subjected to complex loading histories.

5.3. Application and verification

The elastoplastic responses of 316 stainless steel subjected to typical proportional and biaxially non-proportional strain cycling are analyzed. The material has a face-centered-cubic (FCC) crystal lattice. In the local coordinate system, the **n** and **s** of the 12 independent slip systems are listed sequentially in Table 3.

The corresponding numerical algorithm for analyzing the elastoplastic behavior of polycrystalline materials subjected to strain histories is suggested and stated as follows: with the result obtained from the kth iteration of the nth increment of loading, such as $(\Delta\bar{\boldsymbol{\sigma}})_{(n)}^{(k)}$ of the polycrystal, $(\Delta\boldsymbol{\varepsilon}_c)_{(n)}^{(k)}$ and $(\Delta\boldsymbol{\sigma}_c)_{(n)}^{(k)}$ of each single crystal, $(\Delta\gamma^{(m)})_{(n)}^{(k)}$, $(\Delta\varsigma^{(m)})_{(n)}^{(k)}$, and $(\Delta z^{(m)})_{(n)}^{(k)}$ of each slip system, one can compute $[h_{ij}]_{(n)}^{(k)}$ with Eqs. (26), (27) and (2), $[\mathbf{L}_c]_{(n)}^{(k)}$ and $[\mathbf{A}_c]_{(n)}^{(k)}$ for each single crystal with Eqs. (35) and (20) respectively, and then $[\mathbf{L}]_{(n)}^{(k)}$ for the polycrystal with Eq. (39). For the given nth increment of strain $(\Delta\bar{\boldsymbol{\varepsilon}})_{(n)}$, $(\Delta\mathbf{q})_{(n)}^{(k+1)}$ can be obtained using Eq. (20), with which $(\Delta\boldsymbol{\varepsilon}_c)_{(n)}^{(k+1)}$ can be obtained by solving Eq. (22), and then $(\Delta\boldsymbol{\sigma}_c)_{(n)}^{(k+1)}$, $(\Delta\tau_m)_{(n)}^{(k+1)}$ and

Table 3
n and **s** of the 12 independent slip systems of a FCC crystal

	1	2	3	4	5	6	7	8	9	10	11	12
n	$(1\,1\,\bar{1})$	$(1\,1\,\bar{1})$	$(1\,1\,\bar{1})$	$(1\,\bar{1}\,1)$	$(1\,\bar{1}\,1)$	$(1\,\bar{1}\,1)$	$(1\,\bar{1}\,\bar{1})$	$(1\,\bar{1}\,\bar{1})$	$(1\,\bar{1}\,\bar{1})$	$(1\,1\,1)$	$(1\,1\,1)$	$(1\,1\,1)$
s	$[1\,0\,1]$	$[0\,1\,1]$	$[1\,\bar{1}\,0]$	$[1\,1\,0]$	$[0\,1\,1]$	$[1\,0\,\bar{1}]$	$[1\,0\,1]$	$[1\,1\,0]$	$[0\,1\,\bar{1}]$	$[1\,0\,\bar{1}]$	$[0\,\bar{1}\,1]$	$[1\,\bar{1}\,0]$

$(\Delta\gamma_m)^{(k+1)}_{(n)}$ by Eqs. (21), (29) and (31), sequentially. The iterative process continues until the following inequality is satisfied,

$$\delta = \max_{j=1}^{N'} \left[\frac{\left\| \Delta \mathbf{q}^{(k+1)}_{(n)} - \Delta \mathbf{q}^{(k)}_{(n)} \right\|}{\left\| \Delta \mathbf{q}^{(k+1)}_{(n)} \right\|} \right]_j \leqslant \delta_0. \tag{40}$$

After superimposing the derived increments on the corresponding quantities up to the $(n-1)$th increment of loading, one obtains $(\bar{\boldsymbol{\sigma}})_{(n)}$ of the polycrystal, and $(\tau_m)_{(n)}$, $(\varsigma_m)_{(n)}$, $(z_m)_{(n)}$, $(f_m)_{(n)}$, $(H_m)_{(n)}$ of each slip system, and then starts the computation of the next increment of loading. In Eq. (40) δ_0 is the tolerant error, computation shows that $\delta_0 = 0.01$ can satisfy the requirement of both accuracy and computational efficiency.

The responses of 316 stainless steel subjected to cycling along proportional and biaxial nonproportional strain paths at room temperature will be analyzed. The material constants were identified with the experimental result by Tanaka et al. (1985b) and shown in Table 4.

The response of a slip system during a loading–unloading–reloading process is shown in Fig. 2, where the cross-hardening is ignored. The solid line corresponds to the α and C/α given in Table 4; while the dashed line corresponds to $\alpha = 2500$ and $C/\alpha = 0.095$ GPa, i.e., both α and C are reduced to 10% of the values in Table 4. It is seen that, when α is sufficiently large, the constitutive behavior of a slip system predicted with the proposed slip model can be sufficiently close to that with the conventional slip model. With a proper choice of α, the proposed slip model can describe to some extent the Bauschinger effect. For the biaxial loading in the following analysis, the following stress and strain vectors are defined respectively:

$$\vec{\sigma} = \sigma \mathbf{n}_1 + \sqrt{3}\tau \mathbf{n}_2, \quad \vec{\varepsilon} = \varepsilon \mathbf{n}_1 + \frac{1}{\sqrt{3}}\gamma \mathbf{n}_2, \tag{41}$$

where σ and τ denote respectively the axial and the shear stress, ε and γ are the axial and shear strain, $\mathbf{n}_1$ and $\mathbf{n}_2$ are two unit vectors perpendicular to each other. The equivalent stress and strain, σ_e and ε_e, as well as the accumulative strain s are also defined as follows:

Table 4
Material constants

G (GPa)	v	C/α (GPa)	α	d_1	c_1	c_2	c_3	β_s
78.0	0.231	0.0952	25000	1.0	0.0	0.09	0.135	196

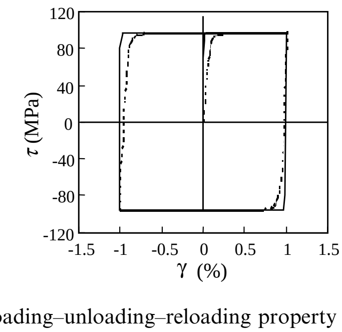

Fig. 2. The loading–unloading–reloading property of a slip system.

$$\sigma_{eq} = |\vec{\sigma}| = \sqrt{\sigma^2 + 3\tau^2}, \quad \varepsilon^{p}_{eq} = |\vec{\varepsilon}^{p}| = \sqrt{(\varepsilon)^2 + \frac{1}{3}(\gamma)^2}, \quad s = \int |d\vec{\varepsilon}|. \tag{42}$$

The responses of the material subjected to symmetrically tensile/compressive strain cycling and pure shear strain cycling with a fixed equivalent strain amplitude $\varepsilon_a = 0.4\%$ are shown in Figs. 3 and 4, respectively. They are in good agreement with the experimental results (Ohashi et al., 1985; Murakami et al., 1989). Compared with the previous analysis (Peng et al., 1997), it can be seen that the hardening that was overpredicted is satisfactorily described by using the new definition for cross-hardening. Distinct difference in the shapes of the hysteresis loops can be observed between these two kinds of strain cycling. On the other hand, the equivalent stress amplitudes corresponding to shear strain cycling is distinctly smaller than that corresponding to the tensile/compressive strain cycling (also see Fig. 7) although the equivalent strain amplitudes are identical. These differences coincide with the experimental observation (Ohashi et al., 1985). These differences can be attributed to the difference of the activated slip systems under these two kinds of loading, which cannot be well described simply by the phenomenological model with Mises equivalent rule.

In the analysis for the response of materials subjected to nonproportional strain cycling, one usually defines the radius of the minimal super-sphere surrounding the strain path as the equivalent strain amplitude ε_a. Figs. 5(b) and 6(b) show, respectively, the computed biaxial stress trajectories corresponding to cyclic strain along a square (Fig. 5(a)) and 90° out-of-phase circular (Fig. 6(a)) paths with $\varepsilon_a = 0.4\%$ in the $\varepsilon - \gamma/\sqrt{3}$ plane, which are in good agreement with the experimental results (Ohashi et al., 1985; Murakami et al., 1989). Compared with the results corresponding to proportional paths (Figs. 3 and 4), the stress

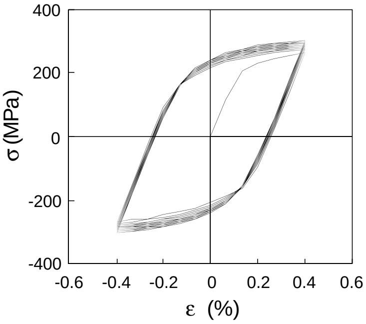

Fig. 3. Computed σ–ε curve under symmetrically tensile/compressive strain cycling with $\varepsilon_a = 0.4\%$.

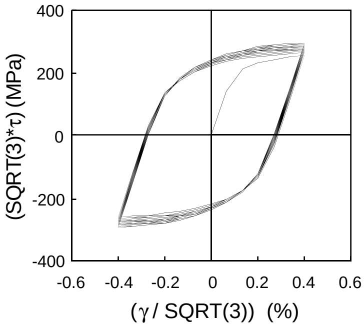

Fig. 4. Computed $\sqrt{3}\tau$–$\gamma/\sqrt{3}$ curve under symmetrically torsional strain cycling with $\varepsilon_a = 0.4\%$.

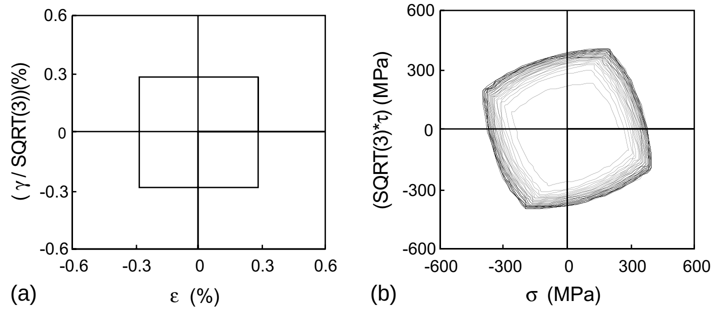

Fig. 5. Response to strain cycling along a square path in ε–$\gamma/\sqrt{3}$ plane with $\varepsilon_a = 0.4\%$. (a) Controlled square strain path in ε–$\gamma/\sqrt{3}$ plane and (b) computed stress trajectory in σ–$\sqrt{3}\tau$ plane.

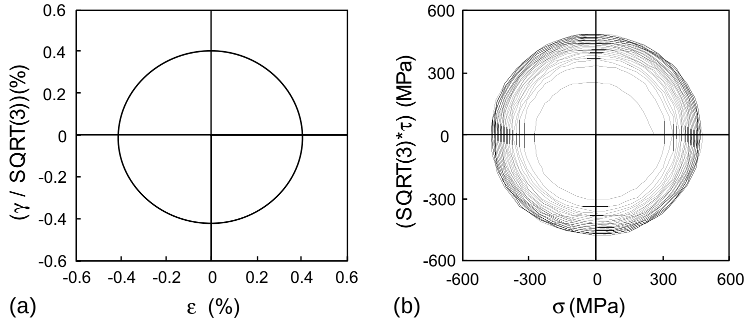

Fig. 6. Response to strain cycling along a circular path in ε–$\gamma/\sqrt{3}$ plane with $\varepsilon_a = 0.4\%$. (a) Controlled square strain path in ε–$\gamma/\sqrt{3}$ plane and (b) computed stress trajectory in σ–$\sqrt{3}\tau$ plane.

amplitudes in Figs. 5 and 6 increase by about 60% (also see Fig. 7), which can be attributed to the nonproportional hardening of the material. In phenomenological analysis, it was usually described by introducing an appropriate definition of nonproportionality and the corresponding hardening rules (Benallel and Marquis, 1987; Fan and Peng, 1991; Tanaka, 1994). However, some fundamental experimental results cannot be well described due to the complicated change in the microstructure. The main features of the 316 stainless steel subjected to typical biaxial nonproportional cycling strain paths are satisfactorily described with the proposed approach and the modified cross-hardening rule.

The variations of the maximum equivalent stress σ_{eq} against the accumulative strain s of the material subjected to cyclic strain along six typical biaxial paths in the ε–$\gamma/\sqrt{3}$ plane with constant strain amplitude $\varepsilon_a = 0.4\%$ are shown in Fig. 7(a), among which, the curves corresponding to cyclic tension/compression and 90° out-of-phase circular paths are in satisfactory agreement with the experimental curves obtained by Murakami et al. (1989), as shown in Fig. 7(b).

As was done by Tanaka et al. (1985b) in the experiment on plastic strain controlled nonproportional cyclic plasticity, the strain paths used in Fig. 7(a) can also be classified into three groups: (1) proportional ones (cyclic tension/compression and cyclic torsion); (2) paths with radiation segments (stellate and cruciform ones); and (3) paths without any segment passes through the origin (square and 90° out-of-phase circular ones). Tanaka et al. (1985b) investigated experimentally the nonproportional cyclic plasticity of 316 stainless steel along these paths in the ε^p–$\gamma^p/\sqrt{3}$ plane with plastic strain amplitude $\varepsilon_a^p = 0.2\%$ and the experimental relationships between σ_{eq} and accumulative plastic strain s^p corresponding to these paths are

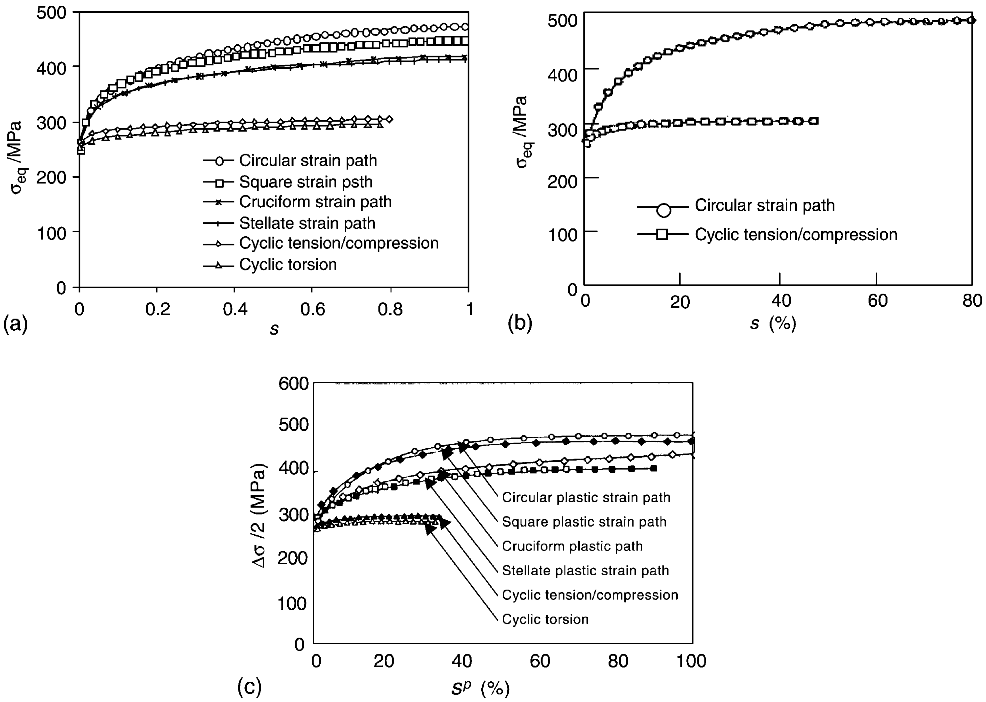

Fig. 7. The relationships between the equivalent stress amplitudes and the accumulated strain or plastic strain along different paths. (a) Computed, strain controlled, (b) experimental, strain controlled (Murakami et al., 1989) and (c) experimental, plastic strain controlled (Tanaka et al., 1985b).

shown in Fig. 7(c) (Tanaka et al., 1985b). Compared with the results by Tanaka, qualitative agreement, in both the saturated values of σ_{eq} and the sequence of curves, can be observed.

6. Conclusions

The following conclusions can be drawn from the above analysis:

(1) The adopted nonclassical hardening law can take into account the contribution of the energy stored in the microstructure of a plastically deformed material to subsequent plastic deformation. It does not use the concept of a critical shear stress and the corresponding slip criterion, which may bring convenience to analysis because it involves no additional process to identify the activation of slip systems and the direction of slip.
(2) Both instantaneous hardening and cross-hardening can be taken into account. A ratio of the energy dissipated on each slip system with respect to the maximum possible dissipated energy without considering cross-hardening was defined and embedded in the Bassani's cross-hardening parameters. It yields a simple cross-hardening rule that proves effective in the description for the nonproportional cyclic plasticity of polycrystalline materials.
(3) The corresponding numerical algorithm based on the Hill's self-consistent scheme and a mixed averaging method was developed for the analysis of elastoplastic responses of polycrystalline materials. The computation shows satisfactory numerical stability, quick convergence and high efficiency.

(4) The cyclic plasticity of 316 stainless steel subjected to cyclic straining along typical proportional and biaxially nonproportional paths was analyzed and the main characteristics were well reproduced. Comparison between the computed and the experimental results showed satisfactory agreement.

Acknowledgements

The authors gratefully acknowledge the financial support to this work from the Natural Science Foundation of China (10272119) and the Education Ministry of China.

Appendix A

The integral of Eq. (6) can be expressed as:

$$\tau^{(m)} = \int_0^{z^{(m)}} C e^{-\alpha(z^{(m)}-z')} \frac{d\gamma^{(m)}}{dz'} dz'. \tag{A.1}$$

Noticing Eqs. (4) and (5) and assuming $H_m = 1$, a bound of the absolute value of $\tau^{(m)}$ can be determined by

$$\begin{aligned} |\tau^{(m)}| &= \left| \int_0^{z^{(m)}} C e^{-\alpha(z^{(m)}-z')} \frac{d\gamma^{(m)}}{dz'} dz' \right| \leqslant \int_0^{z^{(m)}} C e^{-\alpha(z^{(m)}-z')} \left| \frac{d\gamma^{(m)}}{dz'} \right| dz' = C f_m \int_0^{z^{(m)}} C e^{-\alpha(z^{(m)}-z')} dz' \\ &= \frac{C}{\alpha} f_m (1 - e^{-\alpha z^{(m)}}) < \frac{C}{\alpha} f_m. \end{aligned} \tag{A.2}$$

A bound of the dissipation energy $\eta^{(m)}$ (Eq. (11)) on the mth slip system, therefore, can be obtained by

$$\eta^{(m)} = \int_0^{z^{(m)}} \tau^{(m)} \frac{d\gamma^{(m)}}{dz'} dz' \leqslant \int_0^{z^{(m)}} |\tau^{(m)}| \left| \frac{d\gamma^{(m)}}{dz'} \right| dz' < \frac{C}{\alpha} f_m \int_0^{\zeta^{(m)}} d\zeta^{(m)} = \frac{C}{\alpha} f_m \zeta^{(m)}. \tag{A.3}$$

Appendix B

Eqs. (28)–(30) can be expressed in matrix forms as follows:

$$\{\Delta\tau\} = [H]\{\Delta\gamma\} \quad \text{or} \quad \{\Delta\gamma\} = [H]^{-1}\{\Delta\tau\}, \tag{B.1}$$

$$\{\Delta\boldsymbol{\varepsilon}_c^p\} = [\mathbf{P}]\{\Delta\gamma\} \quad \{\Delta\tau\} = [\mathbf{P}]^T\{\Delta\boldsymbol{\sigma}\} \tag{B.2}$$

in which

$$[\mathbf{P}] = [\{\mathbf{p}^1\}, \{\mathbf{p}^2\}, \ldots, \{\mathbf{p}^N\}], \tag{B.3}$$

with

$$\{\mathbf{p}^m\} = \left(p_{11}^m, p_{22}^m, p_{33}^m, 2p_{12}^m, 2p_{23}^m, 2p_{31}^m\right)^T, \tag{B.4}$$

$$\{\Delta\tau\} = (\Delta\tau_1, \Delta\tau_2, \Delta\tau_3, \ldots, \Delta\tau_N)^T, \quad \{\Delta\gamma\} = (\Delta\gamma_1, \Delta\gamma_2, \Delta\gamma_3, \ldots, \Delta\gamma_N)^T, \tag{B.5}$$

$$\{\Delta\boldsymbol{\sigma}_c\} = (\Delta\sigma_{c11}, \Delta\sigma_{c22}, \Delta\sigma_{c33}, \Delta\sigma_{c12}, \Delta\sigma_{c23}, \Delta\sigma_{c31})^T \tag{B.6}$$

and

$$\{\Delta\boldsymbol{\varepsilon}_c^p\} = (\Delta\varepsilon_{c11}^p, \Delta\varepsilon_{c22}^p, \Delta\varepsilon_{c33}^p, 2\,\Delta\varepsilon_{c12}^p, 2\,\Delta\varepsilon_{c23}^p, 2\,\Delta\varepsilon_{c31}^p)^T. \tag{B.7}$$

It can be obtained from Eqs. (B.1) and (B.2) that

$$\{\Delta\boldsymbol{\varepsilon}_c^p\} = [\mathbf{P}][H]^{-1}[\mathbf{P}]^T\{\Delta\boldsymbol{\sigma}_c\}. \tag{B.8}$$

Keeping in mind that

$$\{\Delta\boldsymbol{\varepsilon}_c\} = \{\Delta\boldsymbol{\varepsilon}_c^p\} + \{\Delta\boldsymbol{\varepsilon}_c^e\} \quad \text{and} \quad \{\Delta\boldsymbol{\varepsilon}_c^e\} = [\mathbf{D}^e]^{-1}\{\Delta\boldsymbol{\sigma}_c\}, \tag{B.9}$$

$\{\Delta\boldsymbol{\varepsilon}_c^e\}$ and $[\mathbf{D}^e]$ denoting the increment of elastic strain of a single crystal and the elastic matrix, one obtains

$$\{\Delta\boldsymbol{\sigma}_c\} = [\mathbf{L}_c]\{\Delta\boldsymbol{\varepsilon}_c\}, \tag{B.10}$$

with

$$[\mathbf{L}_c] = \left[[\mathbf{D}^e]^{-1} + [\mathbf{P}][H]^{-1}[\mathbf{P}]^T\right]^{-1}. \tag{B.11}$$

References

Bassani, J.L., 1990. Single crystal hardening. Appl. Mech. Rev. 43 (5), 320–327.

Benallel, A., Marquis, D., 1987. Constitutive equation for nonproportional cyclic plasticity. J. Engng. Mater. Tech. 109, 326–336.

Berveiller, M., Zaoui, A., 1979. An extension of the self-consistent scheme to plastically flowing polycrystals. J. Mech. Phys. Solids 26, 32–344.

Bishop, J.F.W., Hill, R., 1951. A theoretical derivation of the plastic properties of polycrystalline face centered metals. Philos. Mag. 42, 414–427.

Brown, M.W., Miller, K.J., 1982. Two decades of progress in the assessment of multiaxial low-cycle fatigue and life prediction. ASTM STP770, pp. 482–299.

Budiansky, B., Wu, T.T., 1962. Theoretical prediction of plastic strain of polycrystals. In: Proc. 4th US National Congr. Appl. Mech., pp. 1175–1185.

Chaboche, J.L., Rousselier, G., 1983. On the plastic and viscoplastic constitutive equations. J. Pressure Vessel Tech. 105, 153–164.

Fan, J., 1999. A micro/macroscopic analysis for cyclic plasticity of dual-phase materials. J. Appl. Mech. 66, 124–136.

Fan, J., Peng, X., 1991. A physically based constitutive description for nonproportional cyclic plasticity. J. Engng. Mater. Tech. 113, 254–262.

Hill, R., 1965. Continuum micro-mechanics of elastoplastic polycrystals. J. Mech. Phys. Solids 13, 89–101.

Hill, R., 1966. Generalized constitutive relations for incremental deformation of metals and crystals multislip. J. Mech. Phys. Solids 14, 95–102.

Hill, R., Rice, J.R., 1972. Constitutive analysis of elastic–plastic crystals at arbitrary strain. J. Mech. Phys. Solids 20, 401–413.

Hutchinson, J.W., 1970. Elastic–plastic behavior of polycrystalline metals and composites. Proc. Roy. Soc. Lond. A 319, 247–272.

Hwang, K., Sun, S., 1994. Micromechanical modeling of cyclic plasticity. In: Xu, B., Yang, W., (Eds.), Advances in Engineering Plasticity. Proc. 2nd Asia–Pacific Symposium on Engineering Plasticity and its Applications. Int. Academic Publisher, Beijing, pp. 41–48.

Krempl, E., Lu, H., 1987. The hardening and rate-dependent behavior of fully annealed AISI type 316 stainless steel under biaxial in-phase strain cycling at room temperature. J. Engng. Mater. Tech. 106, 376–382.

Kroner, E., 1961. Zur plastischen verformung des Vielkrystalls. Acta Metall. 9, 155.

Lin, T.H., 1957. Analysis of elastic and plastic strains of face-centered cubic crystal. J. Mech. Phys. Solids 5, 143.

McDowell, D.L., 1985. A two surface model for transient nonproportional cyclic plasticity. J. Appl. Mech. 52, 298–308.

McDowell, D.L., 1987. Equation of recent developments in hardening and flow rule for rate-independent nonproportional cyclic plasticity. J. Appl. Mech. 54, 323–334.

Moosbrugger, J.C., McDowell, D.C., 1989. On a class of kinematic hardeningrules for nonproportional cyclic plasticity. J. Engng. Mater. Tech. 111, 87–98.

Murakami, S., Kawai, M., Aoki, K., Ohmi, Y., 1989. Temperature dependence of multiaxial non-proportional cyclic behavior of type 316 stainless steel. J. Engng. Mater. Tech. 111 (1), 32–39.
Ohashi, Y., Tanaka, E., Ooka, M., 1985. Plastic deformation behavior of type 316 stainless steel subjected to out-of-phase strain cycles. J. Engng. Mater. Tech. 107 (4), 286–292.
Ohno, N., 1982. A constitutive model of cyclic plasticity with a nonproportional strain range. J. Appl. Mech. 49, 721–727.
Ohno, N., 1990. Recent topics in constitutive modeling of cyclic plasticity and viscoplasticity. Appl. Mech. Rev. 43 (1), 283–295.
Ohno, N., Kachi, Y., 1986. A constitutive model of cyclic plasticity for nonlinear hardening materials. J. Appl. Mech. 53, 395–403.
Peng, X., Fan, J., 1993. A new numerical approach for nonclassical plasticity. Comput. Struct. 47 (2), 313–320.
Peng, X., Fan, J., 2000. A new approach to polycrystal plasticity. Arch. Mech. 52 (1), 103–125.
Peng, X., Ponter, A.R.S., 1994. A constitutive law for two-phase materials with experimental verification. Int. J. Solids Struct. 31 (8), 1099–1111.
Peng, X., Zeng, X., Fan, J., 1997. On a nonclassical constitutive theory of crystal plasticity. Mech. Res. Commun. 24 (6), 631–638.
Song, Z.R., 1992. The Physics of Metals. High Education Press, Beijing.
Sotolongo, W., McDowell, D.L., 1986. An evaluation of several constitutive model structures for transient nonproportional cyclic plasticity. J. Pressure Vessel Tech. 108, 273–279.
Tanaka, E., 1994. A nonproportionality parameter and a cyclic viscoplastic constitutive model taking into account amplitude dependences and memory effects of isotropic hardening. Eur. J. Mech., A/Solids 13 (2), 155–173.
Tanaka, E., Murakami, S., Ooka, M., 1985a. Effect of plastic strain amplitudes on nonproportional cyclic plasticity. Acta Mech. 57, 167–182.
Tanaka, E., Murakami, S., Ooka, M., 1985b. Effect of strain path shape on nonproportional cyclic plasticity. J. Mech. Phys. Solids 33, 559–575.
Takahashi, H., 1988. Prediction of plastic stress–strain relations of polycrystals based on the Lin's model. Int. J. Plast. 4, 231–247.
Takahashi, H., Motohashi, H., Tokuda, M., Abe, T., 1994. Elastic–plastic finite element polycrystal model. Int. J. Plast. 10 (1), 63–80.
Taylor, G.I., 1938. Plastic strain in metals. J. Inst. Metals 62, 307–324.
Valanis, K.C., 1980. Fundamental consequences on new intrinsic time measure as a limit of endochronic theory. Arch. Mech. 32, 171–190.